The Astrophysical Journal, 580:969–979, 2002 December 1

SELF-SIMILAR CHAMPAGNE FLOWS IN H II REGIONS

Frank H. Shu
National Tsing Hua University, 101 Section 2 Kuang Fu Road, Hsinchu, Taiwan 30013, Republic of China; shu@astron.berkeley.edu

Susana Lizano
Instituto de Astronomía, Universidad Nacional Autónoma de México, Campus Morelia, Apartado 3-72 (Xangari), 58089 Morelia, Michoacán, México; s.lizano@astrosmo.unam.mx

Daniele Galli
Osservatorio Astrofisico di Arcetri, Largo Enrico Fermi 5, I-50125 Florence, Italy; galli@arcetri.astro.it

Jorge Cantó
Instituto de Astronomía, Universidad Nacional Autónoma de México, Apartado 70-264, 4510 México, DF, México

and

Gregory Laughlin
Lick Observatory, University of California, Santa Cruz, CA 95064; laugh@ucolick.org
Received 2002 May 20; accepted 2002 August 1

ABSTRACT

We consider the idealized expansion of an initially self-gravitating, static, singular, isothermal cloud core. For $t \geq 0$, the gas is ionized and heated to a higher uniform temperature by the formation of a luminous but massless star in its center. The approximation that the mass and gravity of the central star are negligible for the subsequent motion of the H II region holds for distances r much greater than $\sim$100 AU and for the massive cloud cores that give rise to high-mass stars. If the initial ionization and heating are approximated to occur instantaneously at $t = 0$, then the subsequent flow (for $r \gg 100$ AU) caused by the resulting imbalance between self-gravity and thermal pressure is self-similar. Because of the steep density profile ($\rho \propto r^{-2}$), pressure gradients produce a shock front that travels into the cloud, accelerating the gas to supersonic velocities in what has been called the "champagne phase." The expansion of the inner region at $t > 0$ is connected to the outer envelope of the now ionized cloud core through this shock, whose strength depends on the temperature of the H II gas. In particular, we find a modified Larson-Penston (L-P) type of solution as part of the linear sequence of self-similar champagne outflows. The modification involves the proper insertion of a shock and produces the right behavior at infinity ($v \rightarrow 0$) for an outflow of finite duration, reconciling the long-standing conflict on the correct (inflow or outflow) interpretation for the original L-P solution. For realistic heating due to a massive young central star that ionizes and heats the gas to $\sim 10^4$ K, we show that even the self-gravity of the ionized gas of the massive molecular cloud core can be neglected. We then study the self-similar solutions of the expansion of H II regions embedded in molecular clouds characterized by more general power-law density distributions: $\rho \propto r^{-n}$ with $3/2 < n < 3$. In these cases, the shock velocity is an increasing function of the exponent n and diverges as $n \rightarrow 3$. We show that this happens because the model includes an origin where the pressure driving the shock diverges because the enclosed heated mass is infinite. Our results imply that the continued photoevaporation of massive reservoirs of neutral gas (e.g., surrounding disks and/or globules) near the embedded ionizing source is required in order to maintain over a significant timescale the emission measure observed in champagne flows.

Subject headings: H II regions — hydrodynamics — ISM: clouds — stars: formation

1. INTRODUCTION

For a spherically symmetric molecular cloud core, initially at rest, the size r_S of the region that can be ionized is given by the standard formula (Strömgren 1939)

$$\int_{r_0}^{r_S} n_e n_p \alpha_2 4\pi r^2 dr = \dot{N}_* \ . \tag{1}$$

Equation (1) assumes ionization equilibrium and the "on the spot" approximation. In the above, n_e is the electron density; n_p is the ion density; α_2 is the recombination coefficient to the second energy level of hydrogen; $\dot{N}_*$ is the rate of ionizing photons from the star, assumed to be a constant; and r_0 is the radius below which all of the gas in the original cloud core can be considered to have fallen into the center (perhaps via a disk) to make a star of mass M_*.[1] If the virial velocity (thermal, turbulent, or magnetohydrodynamic) supporting the original (neutral) cloud core before star formation is denoted by a_1, order-of-magnitude arguments yield $r_0 \sim r_1$, the Bondi-Parker radius of this neutral gas:

$$r_1 \equiv \frac{GM_*}{2a_1^2} \ . \tag{2}$$

The square of the sound speed in the H II gas a_2^2 is generally appreciably larger than a_1^2; thus, the equivalent Bondi-

[1] In the case when $\dot{N}_* \propto t^3$, Newman & Axford (1968) found self-similar solutions for the expansion of an ionization-bounded H II region in a uniform H I cloud.

Parker radius of the ionized gas,

$$r_2 \equiv \frac{GM_*}{2a_2^2} , \tag{3}$$

will be considerably smaller than r_1.

For typical numbers, $M_* \simeq 25\ M_\odot$, $a_1 \simeq 1$ km s^{-1}, and $a_2 \simeq 10$ km s^{-1}, we have $r_1 \simeq 10^4$ AU $\gg r_2 \simeq 10^2$ AU, with both r_1 and r_2 much bigger than the physical radius of the star. Much interior to r_2, the ionized gas will empty into the star (or more likely, into a disk if it has even a slight amount of angular momentum); whereas much exterior to r_2, the gravitationally unbound H II gas will expand outward, if it has not already reached pressure equilibrium with the surrounding cloud. Since $r_0 \gg r_2$, we can henceforth ignore the gravitational field of the star on the flow of the H II region beyond r_0, although for purposes of making contact with earlier theoretical work, we will begin by not ignoring the self-gravity of this gas. Since the material inside r_0 of the initial density profile should have fallen into the star, the observed presence of appreciable amounts of ionized gas at intermediate radii, $\sim 10^3$ AU in typical ultracompact H II regions, is awkward to explain. We defer until § 6 the discussion of the special kinds of models that are probably required to explain ultracompact H II regions.

Assume now that the molecular cloud core initially had a power-law distribution of gas density that extends essentially to infinity:

$$\rho(r) = Kr^{-n} . \tag{4}$$

If $n < 3/2$, the ultraviolet radiation is trapped within a finite radius r_S, and the H II region is said to be "ionization bounded" (see Osterbrock 1989). If $n > 3/2$, the H II region can be either ionization bounded or "density bounded." In the latter case, a finite output of ultraviolet radiation can ionize an infinite volume of gas beyond r_0. The dividing line between being ionization bounded and density bounded arises when the density constant K equals a critical value $K_{\rm cr}$:

$$K_{\rm cr} = 2\mu_i m_{\rm H} \left[\frac{(2n-3) r_0^{2n-3} \dot{N}_*}{4\pi\alpha_2}\right]^{1/2} , \tag{5}$$

where μ_i is the mean weight per particle of the ionized gas, $m_{\rm H}$ is the hydrogen mass, and $n_p = n_e = \rho/2\mu_i m_{\rm H}$.

We wish to compare the value of $K_{\rm cr}$ with the value K_* implied by the assumption that the power law (4) initially extended inward from r_0 as well as outward, but that the part inward of r_0 has fallen into the center (perhaps via a disk) to make a star of mass M_*:

$$K_* = \frac{(3-n)M_*}{4\pi r_0^{3-n}} . \tag{6}$$

Taking the ratio of equation (6) to equation (5), we get

$$\frac{K_*}{K_{\rm cr}} = \left[\frac{(3-n)M_*}{2\mu_i m_{\rm H}}\right] \left[\frac{\alpha_2}{(2n-3)4\pi r_0^3 \dot{N}_*}\right]^{1/2} . \tag{7}$$

For $M_* \simeq 25\ M_\odot$, $r_0 \simeq 10^4$ AU, $\dot{N}_* \simeq 10^{49}$ s^{-1}, $\alpha_2 \simeq 2.6 \times 10^{-13}$ cm^3 s^{-1}, and $K_*/K_{\rm cr} \simeq 23(3-n)/(2n-3)^{1/2}$.

It is remarkable that factors of such disparate orders of magnitude as the dimensionless quantities in the two square brackets of equation (7) combine to give a ratio within 2 orders of unity. Nevertheless, since K_* represents a rough estimate of K and $K_* > K_{\rm cr}$, this calculation formally indicates that the H II regions of 25 $M_\odot$ (and lower mass) stars are likely to be ionization bounded, at least initially, before any expansion occurs. However, if we assume that $\dot{N}_*$ scales roughly as M_*^3 (as indicated by the results of Vacca, Garmany, & Shull 1996), the expression on the right-hand side scales as M_*^{-2}, indicating that the H II regions of the most massive O stars may be density bounded from the start, especially if such stars are born in regions with density gradients close to $n = 3$. They will then develop champagne flows as follows.

When $K \sim K_* < K_{\rm cr}$, the ionization front (IF) created by the idealized instantaneous appearance of a star at $t = 0$ rapidly moves to infinity and establishes an isothermal structure with $T \simeq 10^4$ K. After the passage of the IF, the cloud remains out of mechanical balance, and the pressure gradients will produce an expansion of the whole cloud. Because of the density gradient, the inner regions expand faster than the outer regions, and a shock travels through the cloud, accelerating the gas to supersonic velocities. This is known as the "champagne phase" (e.g., Bodenheimer, Tenorio-Tagle, & Yorke 1979). Franco, Tenorio-Tagle, & Bodenheimer (1990, hereafter FTB) studied the evolution of H II regions embedded in molecular clouds with steep density gradients. High spatial resolution infrared and radio recombination-line observations toward several sources have found ionized gas accelerating away from the central source in the manner expected of champagne flow models (e.g., Garay, Lizano, & Gómez 1994; Keto et al. 1995; Lumsden & Hoare 1996; Lebrón, Rodríguez, & Lizano 2001). Note that in several of the observed compact H II regions (e.g., 29.96−0.02, G32.80+0.19B, G61.48+0.09B1) the inferred rate of ionizing photons implies excitation by central stars with masses $M_* > 30\ M_\odot$.

Density profiles in massive molecular cores have also been extensively studied observationally (e.g., Garay & Rodríguez 1990; Caselli & Myers 1995; Van der Tak et al. 2000; Hatchell et al. 2000; for a review see Garay & Lizano 1999). Even though the environment is possibly clumpy on scales of tenths of parsecs, density profiles are well approximated by power laws with $1 \lesssim n \lesssim 2$. Theoretical models of the formation of massive stars within dense and massive cores have assumed power-law exponents in this range (Osorio, Lizano, & D'Alessio 1999; McKee & Tan 2002). Recently, Franco et al. (2000) have argued that radio continuum spectra of ultracompact H II regions indicate initial density gradients with $2 \lesssim n \lesssim 3$. Clearly, more observations with high spatial resolution are necessary to reliably establish the density profiles of the sites of massive star formation.

The purpose of this paper is to study by similarity techniques the champagne phase of expansion of H II regions with power-law density distributions. In § 2, we formulate the outflow problem in the case of the singular isothermal sphere (SIS) that has $\rho \propto r^{-2}$, including the effect of self-gravity. Tsai & Hsu (1995) found the outflow analog of the inside-out collapse solution (Shu 1977), but in which the SIS is sent into expansion by an outward-propagating shock. In § 3 we show that the Tsai & Hsu (1995) solution is actually the limit of a family of outflow solutions when $(a_1/a_2)^2 \to 1$ from below. Furthermore, the outflow solution with the particular ratio of $(a_1/a_2)^2 = 0.75$ corresponds to a piece of

the time-reversed Larson-Penston (L-P) collapse solution (Larson 1969; Penston 1969), but with a shock inserted to obtain the correct asymptotic behavior for large distances (or early times). For realistic heating after the passage of an IF, i.e., for realistic values of $(a_1/a_2)^2 \ll 1$, we show that the self-gravity of the H II gas can be neglected. In § 4 we extend our study to the evolution of champagne flows in the case of density distributions with power-law exponents in the range $3/2 < n < 3$, neglecting self-gravity. In § 5 we find that the self-similar models have a shock propagating at constant velocity into the ionized gas, in good detailed agreement with the models of FTB. In particular, the shock velocity diverges as $n \to 3$. We show that this happens because the formal treatment extends the inner radius of the calculation to the origin. In such a treatment, the mass of driving H II gas diverges when $n \geq 3$. We perform more realistic calculations in such cases that cut holes in the gas distribution for $r < r_0$. In § 6 we summarize our conclusions, and we discuss the implications of our results for the problem of ultracompact H II regions. Finally, in two appendices we show that, for the scales relevant to molecular cloud cores, the isothermal assumptions for the gas and the shock are valid.

2. GOVERNING EQUATIONS

Consider a star-forming cloud core with the density profile of the SIS

$$\rho(r) = \frac{a_1^2}{2\pi G r^2} , \tag{8}$$

where a_1 is the sound speed of the cloud at $t < 0$. Imagine that at $t = 0$ the central star turns on and heats the entire cloud core to a uniform temperature appreciably higher than it had originally (perhaps by the rapid propagation of an IF). Let $a \equiv a_2 > a_1$ be the sound speed corresponding to this new temperature. In order to keep the initial gas density distribution unchanged from $t = 0^-$ to $t = 0^+$, it is convenient to write

$$\rho(r, 0^+) = \frac{\epsilon a^2}{2\pi G r^2} , \tag{9}$$

where $\epsilon \equiv (a_1/a)^2 \leq 1$. The original temperature was appropriate for a self-gravitating SIS, but the new higher temperature makes the same density distribution overpressured. The gas expands, and a shock front propagates through the cloud, setting it into a champagne outflow.

The expansion of self-gravitating champagne flows is governed by the continuity equation,

$$\frac{\partial \rho}{\partial t} + \frac{1}{r^2}\frac{\partial (r^2 \rho u)}{\partial r} = 0 , \tag{10}$$

where ρ is the gas density and u is the gas velocity, and by the momentum equation,

$$\frac{\partial u}{\partial t} + u\frac{\partial u}{\partial r} = -\frac{a^2}{\rho}\frac{\partial \rho}{\partial r} - \frac{GM}{r^2} , \tag{11}$$

where G is the gravitational constant and M is the mass of the gas inside the radius r. An energy equation is not required since we have assumed an isothermal equation of state $P = a^2\rho$, with shock jumps also occurring isothermally (see Appendix B).

We further simplify the treatment by approximating the central star as a source of light and heat (to keep the gas ionized and warm) but not of mass, and we extend the range of the flow calculation right into the origin. We justify this cavalier treatment of the complex situation interior to $r = r_0$ by noting that the first thing all champagne solutions try to establish is a central region of quasi-uniform pressure (see §§ 3 and 4). All the available ionized mass interior to $r = r_0$ is homogenized by the high pressure in less than a sound crossing time (because supersonic motions are involved), r_0/a. Thus, all detail about the structure of the region interior to $r = r_0$ is lost in a time $\leq 5 \times 10^3$ yr, which is quite short compared to the duration of interest for champagne flows. Apart from initial transients, then, the evolution of quasi-uniform H II regions of high overpressure expanding into exterior regions with power-law density profiles should follow the description given by the self-similar treatment of this paper. An exception to this statement arises if the region interior to $r = r_0$ is a continuous source of additional ionized gas (derived, say, from the *continuous* rather than instantaneous photoevaporation of a circumstellar disk and/or remnant neutral globules). We ignore this exception for the present, but we return to the possibility in § 6 when we comment on the problem of ultracompact H II regions.

2.1. *Similarity Assumption*

Following Shu (1977) we introduce the similarity variable

$$x = \frac{r}{at} , \tag{12}$$

and we define the reduced density

$$\rho(r, t) = \frac{\alpha(x)}{4\pi G t^2} , \tag{13}$$

the reduced mass

$$M(r, t) = \frac{a^3 t}{G} m(x) , \tag{14}$$

and the reduced velocity

$$u(r, t) = a v(x) . \tag{15}$$

Substituting these expressions in equations (10) and (11), one obtains two coupled first-order differential equations for the reduced density α and velocity v,

$$\left[(v - x)^2 - 1\right]\frac{1}{\alpha}\frac{d\alpha}{dx} = \left[\alpha - \frac{2}{x}(x - v)\right](x - v) , \tag{16}$$

$$\left[(v - x)^2 - 1\right]\frac{dv}{dx} = \left[(x - v)\alpha - \frac{2}{x}\right](x - v) , \tag{17}$$

while the reduced mass is given by

$$m = x^2\alpha(x - v) . \tag{18}$$

We identify $t = 0$ as the initial instant and require t, x, m, α, and v all to be positive. Then the critical lines where the left-hand sides and right-hand sides of equations (16) and (17) vanish lie on the locus

$$v_c = x_c - 1, \quad \alpha_c = \frac{2}{x_c} . \tag{19}$$

A special case with an analytical solution that passes

smoothly through the critical line at $x_c = 3$ was cited by Whitworth & Summers (1985, eq. [3.5]):

$$\alpha = \frac{2}{3} , \quad v = \frac{2}{3} x . \tag{20}$$

In dimensional form, this is the model for the Einstein–de Sitter universe (in the nonrelativistic limit where $a^2 \ll c^2$, so that we can ignore the contribution of the gas pressure in determining spacetime curvature), with a Hubble "constant" and cosmic mass density given respectively by $H = 2/3t$ and $\rho = 3H^2/8\pi G = 1/6\pi G t^2$.

In the H II region problem, the reduced central density $\alpha(0) \equiv \alpha_0$ will not usually be tuned to the specific value $\alpha_0 = 2/3$ required to make a smooth crossing of the critical line. Even more, the pressure (and density) homogenization of the central regions cannot extend instantaneously to all space because of the existing density gradient at $t = 0$. Nevertheless, if we ignore the central star (or more accurately, if we put it back to fill the hole inside r_0), the behavior of the Einstein–de Sitter solution is generic for the inner regions of the H II region in that the dimensional central density will decline with time as t^{-2} because of the expansion of the flow toward the exterior regions of lower pressure and density. Thus, for arbitrary values of α_0, we must solve equations (16) and (17) subject to the inner boundary conditions (BCs):

$$\alpha = \alpha_0 , \quad v = 0 \quad \text{at} \quad x = 0 . \tag{21}$$

A series expansion near the origin (a regular singular point of eqs. [16] and [17]) now yields

$$\alpha = \alpha_0 + \frac{\alpha_0}{6}\left(\frac{2}{3} - \alpha_0\right) x^2 + \dots , \tag{22}$$

$$v = \frac{2}{3} x + \frac{1}{45}\left(\frac{2}{3} - \alpha_0\right) x^3 + \dots . \tag{23}$$

The heating of the cloud at $t = 0$ introduces an imbalance between self-gravity and pressure that will induce the propagation of a shock and an outward subsonic flow of the entire system for $t > 0$. We assume isothermal jump conditions

$$(v_u - x_s)(v_d - x_s) = 1 , \quad \frac{\alpha_d}{\alpha_u} = (v_u - x_s)^2 , \tag{24}$$

where the subscript u (d) indicates the value of the reduced velocity and density upstream (downstream) of the shock and x_s is the position (and velocity) of the shock in similarity coordinates. From equation (12) the position and velocity of the shock in physical space are $r_s = x_s a t$ and $u_s \equiv dr_s/dt = a x_s$.

The outer solution to which this shock attaches is given by one of the "plus solutions" of Shu (1977), and it has the asymptotic behavior

$$\alpha \to \frac{2\epsilon}{x^2} , \quad v \to \frac{2(1-\epsilon)}{x} \quad \text{as} \quad x \to \infty , \tag{25}$$

with $\epsilon \leq 1$.

2.2. *Numerical Procedure*

We start the numerical integration of the downstream flow at small x, using the second-order expansions (22) and (23) for a given value of α_0. At each integration point, we apply the isothermal jump conditions, and a provisional upstream solution is obtained. A consistent solution is found when the upstream solution, integrated to large x ($\sim 10^3$), fulfills the asymptotic BCs (25). Thus, for a given α_0 there is a corresponding unique value of ϵ such that the full solution satisfies the BCs (21) and (25) and the jump conditions (24).

3. OUTFLOW SOLUTIONS FOR THE SINGULAR ISOTHERMAL SPHERE

By varying the value of α_0, we obtain a family of outflow solutions. For increasing values of α_0, the shock velocity and shock strength decrease, and the shock attaches to outer solutions characterized by increasing values of $\epsilon \leq 1$. Figure 1 shows the reduced velocity v and density α versus x for $\alpha_0 = 2/3$, 1, 1.67, 4, and 7.90, corresponding to $\epsilon = 0.545$, 0.640, 0.755, 0.916, and 1.

3.1. *The Tsai & Hsu Solution*

There is a maximum value $\alpha_0 = 7.90$ that corresponds to the solution that attaches upstream to the static unperturbed SIS solution with $\epsilon = 1$ (Fig. 1, *thick solid curves*). In this case the shock moves at $u_s = 1.34a$, setting the unperturbed SIS into motion. Since $\epsilon = 1$, the temperature of the cloud has not changed at $t = 0$. Thus, the shock is driven by an infinitesimal pressure pulse at the origin and acquires finite strength as it races down a density gradient. This self-similar solution, found first by Tsai & Hsu (1995), is the outflow counterpart of the "expansion-wave solution" (Shu 1977) for the collapse of the SIS, but now the SIS is sent into expansion by an outwardly propagating shock. Thus, the SIS is unstable not only to self-similar "inside-out collapse" but also to "inside-out expansion" (Tsai & Hsu 1995). (Of course, physically, there is no reason to expect a perturbational heating of the cloud core without having,

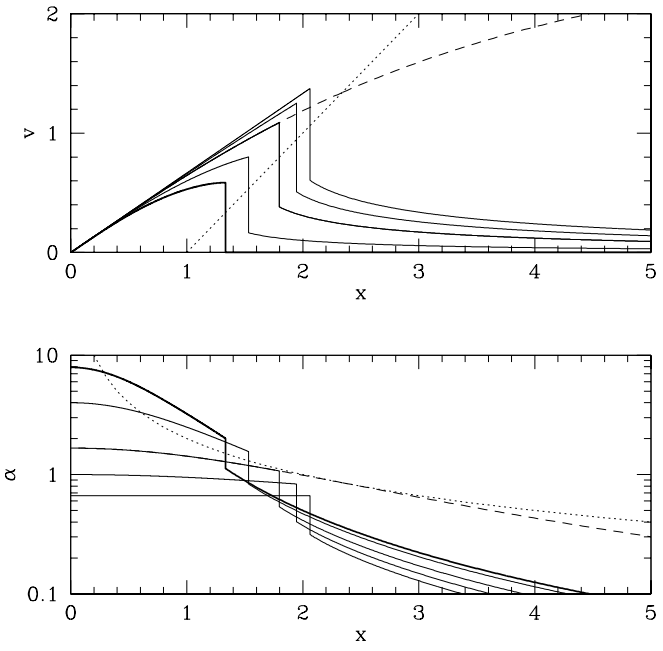

FIG. 1.—*Top*: Reduced velocity v for the outflow solutions of the SIS, including self-gravity. The different curves from top to bottom correspond to $\alpha_0 = 2/3$, 1, 1.67, 4, and 7.90 (*thick solid curve*). The dotted line is the critical line $v = x - 1$. *Bottom*: Reduced density α for the same values of α_0. The dotted curve is the critical line $\alpha = 2/x$. In both panels, the dashed curves show the L-P solution without a shock. The parameters of the solutions are described in Table 1.

first, inward collapse to form a central star.) This special outflow solution is the limit of such solutions as $\epsilon \rightarrow 1$.

3.2. *The Larson-Penston Solution*

For the particular value $\alpha_0 = 1.67$, the flow downstream from the shock front is coincident with a time-reversed piece of the L-P solution originally proposed to describe infall. Without introducing a shock, the L-P solution crosses smoothly the critical lines at $x_c = 2.34$ (Fig. 1, *dotted lines*), the reduced density being tangent to the critical line, and achieves the asymptotic behavior

$$\alpha \rightarrow \frac{8.85}{x^2} , \quad v \rightarrow 3.28 \quad \text{for} \quad x \rightarrow \infty . \tag{26}$$

The L-P solution is represented by dashed curves in Figure 1. In contrast, our outflow solution has a shock at $x_s = 1.80$ and has the asymptotic behavior

$$\alpha \rightarrow \frac{1.50}{x^2} , \quad v \rightarrow 0 \quad \text{for} \quad x \rightarrow \infty , \tag{27}$$

which is less dense than the SIS at large x, as appropriate for an outflow solution. In fact, as discussed by Shu (1977) the time-reversed L-P solution does not represent a proper wind solution, precisely because it is overdense at large radii with respect to the hydrostatic SIS.

3.3. *The Einstein–de Sitter Solution*

For the special case $\alpha_0 = 2/3$, the solution interior to the shock wave at $x_s = 2.06$ is the Newtonian analog to an Einstein–de Sitter ($\Omega = 1$) universe. The pressure (and density, for an isothermal gas) homogenization of the interior is perfect in this case, and Hubble's law of expansion is also exactly satisfied before the gas flow reaches the radius $r = x_s at$. Upstream from the shock front, the flow corresponds to a breeze (see next subsection) blowing slowly through an $\epsilon = 0.545$ SIS. Notice that this use of the Einstein–de Sitter interior solution (connection to an exterior solution via a shock wave) differs from that shown in Figure 1 of Hennebelle (2001; connection via a weak discontinuity).

Unlike its cosmological application, the Einstein–de Sitter (inner) solution represents nothing special in the problem of the self-similar isothermal expansion of self-gravitating H II regions. It merely demarcates the case (see Table 1) when the postshock density α_d switches from values lower than the central level α_0 (for $\alpha_0 > 2/3$) to values higher than the central level (for $\alpha_0 < 2/3$). This switch occurs with increasing heating of the H II gas relative to its neutral precursor [smaller values of $\epsilon \equiv (a_1/a_2)^2$]. With weak heating, running down a density gradient established by the self-gravitating equilibrium of the preionization state and modified by a slowly blowing, upstream breeze counts for more than compression of this gas by a relatively weak shock wave. With strong heating, shock wave compression gains in the competition relative to further propagation into regions of lower density.

3.4. *General Behavior*

With the exception of the inside-out expansion solution of Tsai & Hsu (1995), the upstream flows have $v_u > 0$. This is due to the mechanical imbalance following the heating of the cloud at $t = 0$ causing the gas to expand subsonically before the shock arrives. Such subsonic behavior is characteristic of a "breeze" solution in the nomenclature of the solar-wind literature, and we have referred to it as such. We note, however, that the arrival of the shock wave pushes the breeze into supersonic expansion relative to the origin. The strength of the shock and the value of v_u depend on the new temperature of the cloud at $t = 0^+$. Table 1 summarizes the results for the self-similar models with different values of the central density α_0. The columns are (1) the value of α_0; (2) the parameter ϵ of the upstream solution; (3) the position of the shock, x_s; (4) the postshock velocity v_d; (5) the postshock density α_d; (5) the preshock velocity v_u; and (6) the preshock density α_u. The entries in this table are approximated to three significant figures. The rounding-off error affects the fulfillment of the jump conditions at the level of $\lesssim 2\%$, a sufficient accuracy for practical applications.

3.5. *The Limit* $\epsilon \rightarrow 0$

As discussed in § 2, when the cloud core is heated instantaneously at $t = 0$, the value of ϵ must be chosen for $t = 0^+$ so that the physical density $\rho(r, 0)$ remains unchanged. For a cloud heated by the passage of an IF when a massive star turns on in the center of the core, one expects the equivalent thermal speed to increase from $a_1 \simeq 1$ km s^{-1} to $a \simeq 10$ km s^{-1}. Thus, the value of ϵ for the upstream flow should be quite small, $\epsilon \simeq 10^{-2}$. Since the equilibrium configuration of the cloud has $\epsilon = 1$ for $t < 0$, the condition $\epsilon \ll 1$ implies that

TABLE 1

SINGULAR ISOTHERMAL SPHERE OUTFLOW SOLUTIONS AS A FUNCTION OF α_0

α_0 (1)	ϵ (2)	x_s (3)	v_d (4)	α_d (5)	v_u (6)	α_u (7)
7.90.....	1	1.34	0.586	2	0	1.12
4.....	0.916	1.53	0.801	1.56	0.168	0.835
1.67.....	0.755	1.80	1.09	1.07	0.389	0.539
1.....	0.640	1.95	1.25	0.833	0.513	0.404
2/3.....	0.545	2.06	1.37	2/3	0.605	0.315
0.1.....	0.168	2.42	1.77	0.173	0.905	7.49×10^{-2}
0.01.....	2.09×10^{-2}	2.55	1.90	2.05×10^{-2}	1.00	8.64×10^{-3}
10^{-3}	2.15×10^{-3}	2.56	1.91	2.10×10^{-3}	1.02	8.78×10^{-4}
10^{-4}	2.15×10^{-4}	2.56	1.91	2.10×10^{-4}	1.02	8.80×10^{-5}
10^{-5}	2.15×10^{-5}	2.56	1.91	2.10×10^{-5}	1.02	8.80×10^{-6}

self-gravity is not very important in the subsequent evolution of the cloud for $t > 0$.

We find that as $\epsilon \to 0$, the reduced velocity v converges to an invariant solution with the fastest and strongest shock. Table 1 shows that most flow properties have converged pretty much to their limiting values when $\epsilon \simeq 10^{-2}$. The only formal exception is the reduced density, which converges to a shape-invariant solution that scales as $\alpha_0 \to 0.47\epsilon$. Thus, in the limit $\epsilon \to 0$, we find it convenient to rescale the density as

$$R(x) = \frac{x^2\alpha(x)}{2\epsilon} \ . \tag{28}$$

The physical density for $t > 0$ in term of R is given now by

$$\rho(r, t) = \frac{\epsilon a^2}{2\pi G r^2} R(x) \ . \tag{29}$$

Comparison with equation (9) shows that $R = 1$ at $t = 0^+$.

The top panel of Figure 2 shows the reduced velocity v in the limit $\epsilon = 0$. The position of the shock front is at $x_s = 2.56$, and the upstream reduced velocity, due to the cloud general expansion, is $v_u = 1.02$. The dotted line shows the locus of the critical line (eq. [19]). The bottom panel of Figure 2 shows the reduced density R. The dashed curve shows the function $R = 3(x/x_s)^2$, which corresponds (see eq. [29]) to a region of uniform but steadily decreasing density,

$$\rho(t) = \frac{3}{x_s^2} \frac{\epsilon}{2\pi G t^2} \ , \tag{30}$$

given by spreading the original gaseous mass interior to $r_s = x_s at$ evenly over the enclosed spherical volume. Except for a slight increase of R from its average interior value of 3 to the postshock value $R_d = 3.20$ just downstream from the shock front at $x = x_s$, Figure 2 shows that the high gaseous pressure does a fairly good job of ironing out pressure differences in the interior volume.

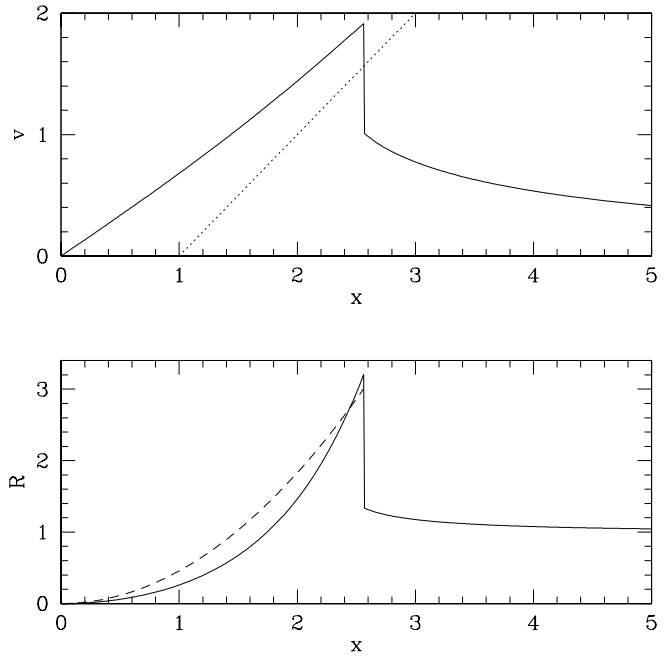

FIG. 2.—*Top*: Reduced velocity v for the exponent $n = 2$, in the limit $\epsilon = 0$. The dotted line is the critical line $v = x - 1$. The shock front is at $x_s = 2.56$. The preshock velocity is $v_1 = 1.02$. *Bottom*: Reduced density R. The dashed curve corresponds to $R = 3(x/x_s)^2$ and shows the deviation from uniform density.

In summary, for a density distribution in mechanical equilibrium at $t < 0$, which comes out of balance at $t = 0^+$ because it has been heated suddenly to a temperature much higher than the original value, one expects that the effects of self-gravity can be neglected with respect to thermal pressure. In this limit where $\epsilon \to 0$, we verify explicitly that the self-similar solution converges to a unique solution, equivalent to the gravitationless case, $G = 0$. Thus, in the next section we will formulate the problem of self-similar champagne flow solutions for power laws of the gas density distribution different from $n = 2$ also in the limit of negligible self-gravity.

4. GENERALIZED FORMULATION IGNORING SELF-GRAVITY OF THE IONIZED GAS

In this section we discuss the champagne flows associated with generalized power-law density profiles with $\rho \propto r^{-n}$ in the limit where the self-gravity of the cloud can be neglected. For $t < 0$, these density profiles result from equilibrium between the self-gravity of the cloud core and other forces in addition to thermal pressure (see, e.g., the discussion on polytropic clouds in Galli et al. 1999). We assume that after heating at $t = 0$, thermal pressure will dominate over such forces in the evolution of the cloud. The governing equations are given by equations (10) and (11), setting $G = 0$. We choose the same self-similar variable and reduced velocity defined by equations (12) and (14), but we generalize the density profile of equation (4) as

$$\rho(r, t) = \frac{K}{r^n} R(x) \ . \tag{31}$$

The nondimensional equations are

$$[(v - x)^2 - 1] \frac{dR}{dx} = \frac{R}{x} [v(v - x)(n - 2) - n] \ , \tag{32}$$

$$[(v - x)^2 - 1] \frac{dv}{dx} = \frac{2v}{x} - n \ . \tag{33}$$

For $x \to \infty$, the boundary conditions are $v \to 0$ and $R \to 1$. Then the asymptotic expansions are

$$v \to \frac{n}{x} \ , \quad R \to 1 + \frac{n(n-1)}{2x^2} \quad \text{for} \quad x \to \infty \ . \tag{34}$$

At the origin,

$$v \to \frac{n}{3} x \ , \quad R \propto x^n \quad \text{for} \quad x \to 0 \ . \tag{35}$$

This boundary condition on R implies that as $r \to 0$ the density is uniform and is only a function of time, $\rho \propto t^{-n}$. This is the expected behavior of the central zone of the H II region, where the sound crossing time is smaller than the expansion time.

We apply the isothermal jump conditions (24) to connect the upstream and downstream solutions. Since the equation for the reduced velocity is now decoupled from the equation for the reduced density, a simple way to find the position of the shock front, x_s, is to integrate numerically equation (33)

outward from $x = 0$ and integrate inward from a large x. We check every point of the downstream solution until the jump condition in the velocity (24) is fulfilled.

Once the reduced velocity v is known, the density equation (32) can be integrated as

$$R(x) = R_b \exp \int_{x_b}^{x} \frac{1}{x'} \frac{v(v - x')(n - 2) - n}{(v - x')^2 - 1} dx' . \quad (36)$$

For the outer solution, $x_b = \infty$ and $R_b = 1$. For the inner solution, $x_b = x_s$ and $R_b = R_d$, where R_d is the downstream reduced density evaluated from the jump condition (24).

Before proceeding to discuss the self-similar champagne flows, let us examine the case $n = 3$. In this case, equations (32) and (33) have the analytic solution $R = Cx^3$ and $v = x$, where C is an arbitrary constant. The jump conditions (24) imply that $x_s \to \infty$ as $v_d \to x$. Thus, in spatial coordinates the shock front, $r_s = x_s at$, and the shock velocity, $u_s = a x_s$, go to infinity.

In dimensional variables, the analytic solution for the case $n = 3$ simply corresponds to a Hubble flow in a $\Omega = 0$ universe: $u = r/t$, $\rho \propto t^{-3}$. The propagation of the shock wave to infinity leaves behind it an expanding H II region of uniform but ever decreasing density that looks like a "little bang." We will discuss below the physical meaning (or lack of it) of this remarkable result.

5. OUTFLOW SOLUTIONS FOR DIFFERENT GRADIENTS

The nongravitating case for $n = 2$ was shown in Figure 2. Figure 3 shows the analogous reduced velocity v and density R for $n = 2.99$. The dotted line in the top panel corresponds to the critical line. In this case the shock front is at $x_s = 19.25$. This number is also the velocity of the shock wave relative to the isothermal speed of sound of the H II region. In contrast, the preshock velocity of the gas (relative to the origin) is only $v_u = 0.16$, because at a given spatial position there is less time for the cloud to expand before the shock arrives. The reduced density R in the bottom panel has a correspondingly large postshock density increase. The dashed curve shows the function

$$R = \frac{3}{3 - n} \left(\frac{x}{x_s} \right)^n , \quad (37)$$

given by spreading the original gaseous mass interior to $r_s = x_s at$ evenly over the enclosed spherical volume. Figure 3 shows that the shock dynamics raise the immediate downstream value from the average expectation $3/(3 - n) = 300$ at $x = x_s$ to the actual postshock value $R_d = 368$.

Table 2 summarizes the results for the self-similar models with different exponents n in the density profile. The columns are (1) the exponent n; (2) the position of the shock, x_s; (3) the postshock velocity v_d; (4) the postshock density R_d; (5) the preshock velocity v_u; and (6) the preshock density R_u. One can see that x_s increases as $n \to 3$.

Figure 4 shows the comparison of our self-similar solutions with the numerical results obtained by FTB in the case $n = 1.7$. We converted the values of the velocity and density calculated by FTB at $t = 1.72 \times 10^5$ yr (see their Fig. 3*c*) into our self-similar variables (eqs. [12], [15], and [31]) using their values of the sound speed and their normalization for the density profile. Figure 4 shows the excellent agreement between their numerical simulation and our similarity calculation.

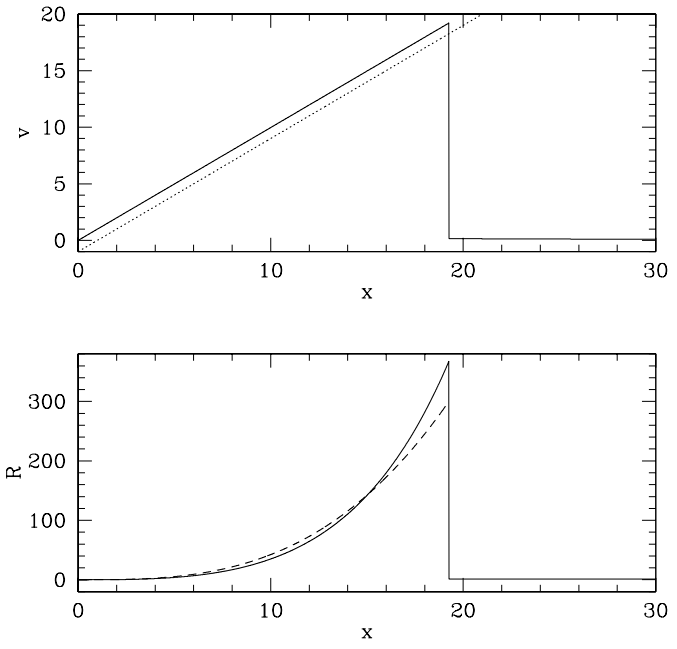

FIG. 3.—*Top*: Reduced velocity v for the exponent $n = 2.99$. The dotted line is the critical line $v = x - 1$. The shock front is at $x_s = 19.25$. The preshock velocity is only $v_1 = 0.16$. *Bottom*: Reduced density R. The dashed curve corresponds to $R = 300(x/x_s)^{2.99}$ and shows the deviation from uniform density.

5.1. *Analytic Approximation*

Following FTB we compare the results of the self-similar champagne flows with a simple analytic approximation.

TABLE 2
FLOW PARAMETERS AS A FUNCTION OF n

n (1)	x_s (2)	v_d (3)	R_d (4)	v_u (5)	R_u (6)
1.5.....	2.15	1.33	1.85	0.93	1.25
1.6.....	2.23	1.44	2.04	0.96	1.28
1.7.....	2.30	1.55	2.26	0.98	1.30
1.8.....	2.38	1.66	2.52	1.00	1.32
1.9.....	2.47	1.78	2.83	1.01	1.33
2.0.....	2.56	1.91	3.20	1.02	1.34
2.1.....	2.66	2.05	3.65	1.01	1.35
2.2.....	2.77	2.21	4.21	1.00	1.34
2.3.....	2.91	2.39	4.93	0.98	1.33
2.4.....	3.07	2.59	5.87	0.95	1.31
2.5.....	3.27	2.85	7.17	0.91	1.29
2.6.....	3.55	3.17	9.10	0.85	1.25
2.7.....	3.96	3.64	12.26	0.76	1.20
2.8.....	4.67	4.42	18.48	0.65	1.14
2.9.....	6.33	6.16	36.94	0.47	1.08
2.95.....	8.76	8.65	73.73	0.34	1.04
2.99.....	19.25	19.20	367.57	0.16	1.01

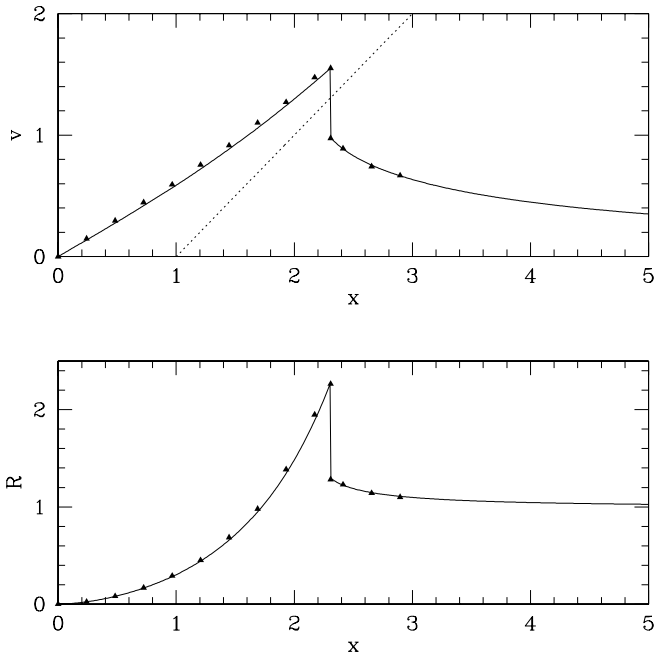

FIG. 4.—*Top*: Reduced velocity v for the exponent $n = 1.7$. The dotted line is the critical line $v = x - 1$. The shock front is at $x_s = 2.30$. The preshock velocity is $v_u = 0.98$. *Bottom*: Reduced density R. In both panels, the triangles show the results of the numerical models of FTB for $n = 1.7$ at $t = 1.72 \times 10^5$ yr, expressed in our self-similar variables.

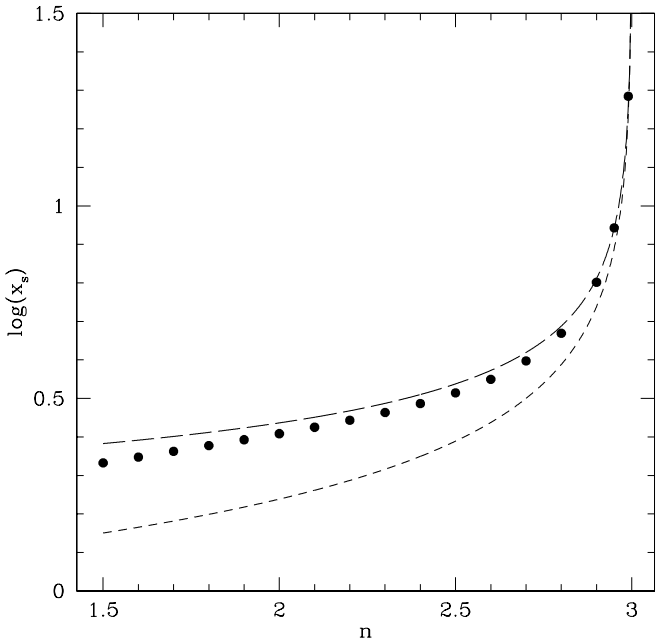

FIG. 5.—Plot of x_s vs. n showing the divergence of the shock position as $n \to \infty$. The dots represent the exact self-similar solutions. The long-dashed curve and the short-dashed curve correspond to the analytic approximation (41) with $u_u = a$ and $u_u = 0$, respectively.

Assume that the pressure driving the shock is uniform,

$$P(t) = a^2 \overline{\rho}(t) \ , \tag{38}$$

where $\overline{\rho}(t)$ is the mean density at a given time; i.e.,

$$\overline{\rho}(t) = \frac{\int_0^{r_s} 4\pi r^2 \rho(r,t) dr}{\int_0^{r_s} 4\pi r^2 dr} = \frac{3}{3-n} \rho[r_s(t)] \quad \text{with} \quad n < 3 \ , \tag{39}$$

where $r_s(t)$ is the instantaneous position of the shock front. This must be equal to the (strong shock) postshock pressure given by

$$P(t) = (u_s - u_u)^2 \rho[r_s(t)] \ , \tag{40}$$

where u_u is the upstream velocity at the position of the shock front. Equating these two pressures, one obtains

$$x_s = \frac{u_s}{a} = \sqrt{\frac{3}{3-n}} + \frac{u_u}{a} \ , \tag{41}$$

which is equivalent to equation (24) of FTB when $u_u = a$. Equation (41) diverges as $n \to 3$ because, in this limit, the mass inside any radius diverges if the origin is included (eq. [39]).

Figure 5 shows $\log(x_s)$ versus n for the self-similar models. The long-dashed curve corresponds to equation (41) where we have used $u_u = a$ (as in FTB). The short-dashed curve instead is equation (41) with $u_u = 0$. The difference is due, in part, to the pressure driving the shock being not exactly uniform as was assumed in the approximation above. The deviation from uniform density was commented on in §§ 3 and 5 when we discussed the approximate nature of the fits provided by the dashed lines in the lower panels of Figures 2 and 3.

To avoid the divergence at the origin, one could integrate from the radius of influence r_0 (or include a uniform core as considered by FTB). In that case, the density can be evaluated for all n and is given by

$$\overline{\rho}(t) = f[r_s(t)] \rho[r_s(t)] \ , \tag{42}$$

where

$$f[r_s(t)] = \begin{cases} \dfrac{3}{3-n} \dfrac{1}{\Omega} \left\{ 1 - [r_0/r_s(t)]^{3-n} \right\} & n \neq 3 \ , \\ \dfrac{1}{\Omega} \ln[r_s(t)/r_0]^3 & n = 3 \ , \end{cases} \tag{43}$$

and $\Omega = 1 - [r_0/r_s(t)]^3$ is a volume factor. The shock velocity is then

$$u_s = a \sqrt{f[r_s(t)]} + u_u \ . \tag{44}$$

For $n < 3$, $f(r_s) \to 3/(3-n)$ when $r_s \gg r_0$; thus, the shock reaches the asymptotic constant value given by equation (41). For the case $n \geq 3$, the shock accelerates to ∞ as $r_s \to \infty$. The latter divergence arises only because a shock wave of finite outward momentum is allowed to run into spherical shells of ever decreasing mass.

Finally, as discussed in Appendices A and B, even though the expansion velocities become very large as $n \to 3$, adiabatic cooling never offsets photoionization heating, and the gas remains isothermal. We also show that for the scales of interest in molecular clouds, even if the shock velocity becomes large, the assumption of an isothermal shock remains valid.

6. DISCUSSION

Compact H II regions with velocity gradients indicative of champagne flows are characterized by values of the emission measure (EM) in the range 10^6 cm^{-6} pc $\lesssim$ EM $\lesssim 10^8$ cm^{-6} pc (e.g., Garay et al. 1994). The results of FTB and the self-similar models presented here show that when a molecular core is ionized and heated out of equilibrium, steep density gradients characteristic of star-forming regions produce shocks that travel at constant velocity and accelerate the ionized gas to supersonic speeds. This phase of supersonic expansion of the ionized gas poses a lifetime problem for champagne flows, more severe than the one pointed out by Wood & Churchwell (1989) in the case of ultracompact H II regions.

The emission measure of the self-similar models presented here at time $t = 0^+$, just after ionization of the cloud core, is

$$\mathrm{EM}_0 \equiv \int_{r_0}^{\infty} n_e n_p \, dr = \frac{1}{2n-1}\left(\frac{K}{2\mu_i m_{\mathrm{H}}}\right)^2 r_0^{1-2n} . \quad (45)$$

As we discussed in § 1, if $K < K_{\mathrm{cr}}$, the H II region is density bounded and therefore able to develop a champagne flow. With K_{cr} defined by equation (5) and our fiducial values of the physical parameters for a 25 $M_\odot$ star, this condition results in the following upper limit on the EM:

$$\mathrm{EM}_0 < \frac{2n-3}{2n-1}\frac{\dot{N}_*}{4\pi\alpha_2 r_0^2} \sim 4 \times 10^7 \text{ cm}^{-6} \text{ pc} , \quad (46)$$

in the middle of the range indicated by the observations. However, inserting the expression of $\rho(r, t)$ given by equation (31) into the equation (45), one easily obtains $\mathrm{EM}(t) \propto t^{1-2n}$ for $t \gg r_0/a$. Thus, the expansion of the champagne flows results in a rapid decrease of the emission measure, and in a short time the source fades away from observational classification as a compact H II region. Inclusion of the effects of a fast stellar wind would only exacerbate the situation.

These estimates show that a continuous source of ionized mass is required to keep up the density of the expanding champagne flow. Photoevaporation of circumstellar disks (Hollenbach et al. 1994; Richling & Yorke 1997) or mass loading by the photoevaporation and/or hydrodynamic ablation of remnant neutral globules surrounding the central star (e.g., Lizano et al. 1996; Redman, Williams, & Dyson 1996) are natural solutions for maintaining the high observed emission measures in champagne flows and, in general, in ultracompact H II regions. In particular, proplyds in Orion, sites of low-mass star formation, are known to have appreciable mass-loss rates that can mass-load the stellar wind (Störzer & Hollenbach 2000; García-Arredondo, Arthur, & Henney 2002). Revealed O and B stars show a lower frequency of surrounding disks than stars of spectral type A and later (Natta, Grinin, & Mannings 2000; Lada et al. 2000), suggestive of a picture where the disks are photoevaporated during an earlier phase of evolution, perhaps as ultracompact H II regions. As a first attempt to model quasi-spherical ultracompact H II regions on this basis, it would be interesting to extend the methods of this paper to include a continuous source of ionized gas (due to photoevaporation of a disk or neutral globules into a mass-loaded stellar wind) that emanates at a prescribed rate and speed from the origin.

7. CONCLUSIONS

We have obtained self-similar champagne flow solutions for the expansion of power-law gas density distributions after the gas has been uniformly heated out of mechanical equilibrium by the birth of a star at the center of a molecular cloud core. These solutions attach via a shock to upstream breeze solutions.

In the case of the isothermal sphere with $\rho \propto r^{-2}$, the "inside-out expansion" found by Tsai & Hsu (1995) is the limit of the family of self-similar outflow solutions when the sound speed a_2 of the H II region is the same as the sound speed a_1 of the original molecular cloud core. The case $(a_1/a_2)^2 = 1$ must include the effect of the self-gravity of the gas, and the outflow solution then attaches to the unperturbed static SIS upstream of the shock. Another member of this family, for $(a_1/a_2)^2 = 0.75$, is a time-reversed piece of the L-P collapse solution, with a shock allowing the upstream solution to have a correct outflow (breeze) asymptotic behavior.

For the high values of the gas temperature expected after the passage of an IF, $(a_1/a_2)^2 \ll 1$, and the self-gravity of the gas can be neglected. The solution then approaches a shape-invariant form. In the approximation that the self-gravity of the ionized gas can be ignored, we computed the self-similar champagne flows of H II regions formed in molecular clouds characterized by power-law density distributions with exponents $3/2 < n < 3$. These self-similar solutions behave as in the numerical models of FTB: in the "champagne phase," a shock moves with a constant speed into the ionized medium with a shock speed that increases with increasing density gradient. The speed of the shock diverges as $n \to 3$ because the mass of the driving gaseous piston diverges, if the origin is included. Instead, if the origin is excluded, the shock front velocity reaches an asymptotic constant value for $n < 3$. For $n \geq 3$ the shock accelerates to infinite velocity as $r_s \to \infty$, but only because finite outward momentum is inputted into spherical shells of ever decreasing mass. These results may help explain astrophysical champagne flows where expansion velocities are seen that are considerably larger than the sound speed $a_2 \simeq 10$ km s^{-1} associated with conventional H II regions. (Driving by fast stellar winds may contribute to the perceived motions.) Despite the large expansion velocities produced in the case of the steepest pressure gradients ($n \to 3$), we show in two appendices that the isothermal assumption for the gas and for the shock are valid for the scales of interest in molecular clouds.

The supersonic expansion of the ionized gas creates a severe lifetime problem for champagne flows. A natural solution is the photoevaporation of circumstellar disks and/or remnant neutral globules, which would help maintain the high observed emission measures in these sources.

We thank Luis Rodríguez, Malcolm Walmsley, and Frank Wilkin for useful comments on the manuscript. F. S. acknowledges support in the United States from the NSF and NASA and in Taiwan from the National Science Council. S. L. and J. C. acknowledge support from DGAPA/UNAM and CONACyT. D. G. acknowledges support from grant COFIN-2000 and warm hospitality from the Instituto de Astronomía, UNAM, in Morelia.

APPENDIX A

ADIABATIC COOLING VERSUS PHOTOIONIZATION HEATING

For an expanding nebula, the equilibrium temperature is given by the balance between photoionization heating $\Gamma_{\rm ph}$ and radiative cooling $\Lambda_{\rm rad}$ and adiabatic cooling $\Lambda_{\rm ad}$.

We can estimate when adiabatic cooling becomes important by setting

$$\Gamma_{\rm ph} = \Lambda_{\rm ad} \ . \tag{A1}$$

Assuming ionization equilibrium and the "on the spot" approximation, $\Gamma_{\rm ph}$ is given by

$$\Gamma_{\rm ph} \simeq n_e n_p \alpha_{2\frac{3}{2}} kT_* \ , \tag{A2}$$

where T_* is the stellar temperature (e.g., Osterbrock 1989). The rate of adiabatic cooling (for a constant mass) is given by

$$\Lambda_{\rm ad} = \frac{P}{V}\frac{dV}{dt} = a^2 \left| \frac{d\overline{\rho}}{dt} \right| \ . \tag{A3}$$

Then the condition for adiabatic cooling to win over photoionization heating can be written as

$$\frac{t_{\rm rec}}{t_\rho} \geq \frac{3}{4}\frac{T_*}{T} \ , \tag{A4}$$

where $t_{\rm rec} \equiv 1/n_e\alpha_2$ is the recombination timescale and $t_\rho \equiv \overline{\rho}/|d\overline{\rho}/dt|$ is the timescale for the decrease in the density.

Taking $T_*/T \simeq 4$, the critical ratio of timescales is

$$\frac{t_{\rm rec}}{t_\rho} \simeq 3 \ . \tag{A5}$$

On the other hand, using equations (31) and (39), this ratio can be written as

$$\frac{t_{\rm rec}}{t_\rho} = 2n\frac{3-n}{3}\frac{\mu_i m_{\rm H} a}{K\alpha_2} x_s r_s^{n-1} \ . \tag{A6}$$

Using the critical value for the ratio of timescales (A5), one can solve this equation for a critical radius $r_{\rm cr}$ beyond which the isothermal assumption breaks down. For convenience, one can write the density constant in equation (4) as $K = \mu m_{\rm H} n_0 r_0^n$, where μ is the mean molecular weight and n_0 is the number density at the distance r_0. Then the critical radius can be written as

$$r_{\rm cr} = r_0 \left(\frac{\alpha_2 \mu n_0 r_0}{2\mu_i a x_s} \frac{3}{3-n}\frac{3}{n} \right)^{1/(n-1)} \ . \tag{A7}$$

Finally, for $\alpha_2 \simeq 2.6 \times 10^{-13}$ cm^3 s^{-1} and the fiducial parameters $n_0 \simeq 10^4$ cm^{-3}, $r_0 \simeq 10^4$ AU, $a \simeq 10$ km s^{-1}, and $\mu \simeq 2$, typical of massive molecular cloud cores, the critical radius becomes

$$r_{\rm cr} \simeq r_0 \left[780 \left(\frac{3}{3-n} \right)^{1/2} \frac{3}{n} \right]^{1/(n-1)} \ , \tag{A8}$$

where we used equation (41) with $u_u = 0$ to obtain the last expression.

This critical radius is large compared to r_0 and the sizes of molecular cloud cores where the stars are formed. Thus, adiabatic cooling never dominates over photoionization heating, and the assumption of an isothermal gas is justified.

APPENDIX B

ISOTHERMAL SHOCK

We now examine the assumption that the shock is isothermal in the case when the shock speed is large ($n \rightarrow 3$). The post-shock temperature is

$$T_d \simeq \frac{3}{16}\frac{\mu_i m_{\rm H}}{k} u_s^2 = 1.2 \times 10^3 \left(\frac{u_s}{10 \text{ km s}^{-1}} \right)^2 \text{ K} \ . \tag{B1}$$

For large shock velocities the gas behind the shock will not be able to cool efficiently; thus, the cooling time may become larger

than the expansion time, $t_{\rm cool} > t_{\rm exp} = r_s/u_s$, and the shock may become energy conserving.

The expansion time is

$$t_{\rm exp} = 1.5 \times 10^{11} \frac{r}{10^4 \text{ AU}} \left(\frac{u_s}{10 \text{ km s}^{-1}} \right)^{-1} \text{ s} . \tag{B2}$$

The cooling time is given by

$$t_{\rm cool} = \frac{3}{2} \frac{kT_d}{n_d \Lambda_{\rm rad}} , \tag{B3}$$

where T_d is the gas postshock temperature, n_d is the gas postshock number density, and $\Lambda_{\rm rad}$ is the cooling function (in ergs cm^3 s^{-1}). Substituting the postshock temperature (B1), using equation (24) for the postshock density, and assuming that the upstream flow is as rest, the cooling time can be rewritten as

$$\begin{aligned} t_{\rm cool} &= \frac{9\mu_i^2 m_{\rm H} a^2}{32\mu} \frac{1}{n_0 \Lambda_{\rm rad}} \left(\frac{r_s}{r_0} \right)^n \\ &\simeq 1.4 \times 10^4 \left(\frac{\Lambda_{\rm rad}}{10^{-23} \text{ ergs cm}^3 \text{ s}^{-1}} \right)^{-1} \left(\frac{r_s}{10^4 \text{ AU}} \right)^n \text{ s} , \end{aligned} \tag{B4}$$

where we have again used the expression for K defined in Appendix A.

Thus, the ratio is

$$\frac{t_{\rm cool}}{t_{\rm exp}} \simeq 10^{-7} \left(\frac{\Lambda_{\rm rad}}{10^{-23} \text{ ergs cm}^3 \text{ s}^{-1}} \right)^{-1} \left(\frac{r_s}{10^4 \text{ AU}} \right)^{n-1} \frac{u_s}{10 \text{ km s}^{-1}} . \tag{B5}$$

This equation is expressed in terms of typical values of the cooling function (e.g., Dalgarno & McCray 1972) and shows that the ratio of cooling time to expansion time is small. Thus, the assumption of an isothermal shock will remain valid for the scales relevant in molecular clouds.

REFERENCES

Bodenheimer, P., Tenorio-Tagle, G., & Yorke, P. 1979, ApJ, 233, 85
Caselli, P., & Myers, P. 1995, ApJ, 446, 665
Dalgarno, A., & McCray, R. A. 1972, ARA&A, 10, 375
Franco, J., Kurtz, S., Hofner, P., Testi, L., García-Segura, G., & Martos, M. 2000, ApJ, 542, L143
Franco, J., Tenorio-Tagle, G., & Bodenheimer, P. 1990, ApJ, 349, 126 (FTB)
Galli, D., Lizano, S., Li, Z.-Y., Adams, F. C., & Shu, F. H. 1999, ApJ, 521, 630
Garay, G., & Lizano, S. 1999, PASP, 111, 1049
Garay, G., Lizano, S., & Gómez, Y. 1994, ApJ, 429, 268
Garay, G., & Rodríguez, L. F. 1990, ApJ, 362, 191
García-Arredondo, F., Arthur, J., & Henney, W. 2002, Rev. Mexicana Astron. Astrofis., 38, 51
Hatchell, J., Fuller, G. A., Millar, T. J., Thompson, M. A., & Macdonald, G. H. 2000, A&A, 357, 637
Hennebelle, P. 2001, A&A, 378, 214
Hollenbach, D., Johnstone, D., Lizano, S., & Shu, F. H. 1994, ApJ, 428, 654
Keto, E. R., Welch, W. J., Reid, M. J., & Ho, P. T. P. 1995, ApJ, 444, 765
Lada, C. J., Muench, A. A., Haisch, K. E., Lada, E., Alves, J. F., Tollestrup, E. V., & Willner, S. P. 2000, AJ, 120, 3162
Larson, R. B. 1969, MNRAS, 145, 271
Lebrón, M., Rodríguez, L. F., & Lizano, S. 2001, ApJ, 560, 806
Lizano, S., Cantó, J., Garay, G., & Hollenbach, D. 1996, ApJ, 468, 739
Lumsden, S. L., & Hoare, M. G. 1996, ApJ, 464, 272
McKee, C., & Tan, J. C. 2002, Nature, 416, 59
Natta, A., Grinin, V. P., & Mannings, V. 2000, in Protostars and Planets IV, ed. V. Mannings, A. P. Boss, & S. S. Russell (Tucson: Univ. Arizona Press), 559
Newman, R. C., & Axford, W. I. 1968, ApJ, 153, 595
Osorio, M., Lizano, S., & D'Alessio, P. 1999, ApJ, 525, 808
Osterbrock, D. E. 1989, Astrophysics of Gaseous Nebulae and Active Galactic Nuclei (Mill Valley: University Science Books)
Penston, M. V. 1969, MNRAS, 144, 425
Redman, M. P., Williams, R. J. R., & Dyson, J. E. 1996, MNRAS, 280, 661
Richling, S., & Yorke, H. W. 1997, A&A, 327, 317
Shu, F. 1977, ApJ, 214, 488
Störzer, H., & Hollenbach, D. 2000, ApJ, 539, 751
Strömgren, B. 1939, ApJ, 89, 526
Tsai, J. C., & Hsu, J. J. L. 1995, ApJ, 448, 774
Vacca, W. D., Garmany, C. D., & Shull, J. M. 1996, ApJ, 460, 914
van der Tak, F. F. S., van Dishoeck, E. F., Evans, N. J., II, & Blake, G. A. 2000, ApJ, 537, 283
Whitworth, A., & Summers, D. 1985, MNRAS, 214, 1
Wood, D. O. S., & Churchwell, E. 1989, ApJS, 69, 831